



Electrochemical characterization of rust converter based on phosphoric acid

Xiaodong Zhao^{*1}, Weijie Fan¹, Xiqiu Fan¹, Chablovski Vladimir², Tuchkovskaya Alla²
and Vrubleuskaya Volha²

¹School of Naval Architecture and Ocean Engineering, Zhejiang Ocean University, Zhoushan, China

²Research Institute for Physical and Chemical Problems, Belarusian State University, Minsk, Belarus

ABSTRACT

A rust converter based on phosphoric acid had been designed and analyzed for the corrosion of mild steel in neutral and acid media. The corrosion inhibition efficiency of the converter was evaluated by means of electrochemical techniques such as electrochemical impedance spectroscopy (EIS) and potentiodynamic polarization in comparison with untreated rusty steel at different temperatures. The forming mechanism of the conversion layer was discussed on account of the formula of the converter preparation together with the X-ray analysis results.

Keywords: Rust converter; potentiodynamic polarization; electrochemical impedance spectroscopy (EIS); phosphate

INTRODUCTION

Iron rust can be generally divided in two categories: non-adherent rust (NAR) and adherent rust (AR). Non-adherent rust results from the direct contact between the metal surface and the atmosphere, which is friable, powdery and high impurity-containing but easy to remove by mechanical treatment. While adherent rust generates from the interaction of inner iron and penetrated water, maintaining a high adherent force with substrate thus difficult for removal. The different component and heterogeneous distribution of the latter are responsible for the decrease of the cohesive force between the subsequent painting and base metal as well as the anodic corrosion after the coating deterioration [1]. For a long time, various techniques of surface treatment are employed to prevent from metal corrosion, among which sand blasting provides high level of rust removal and the superior surface with roughness suitable for subsequent anticorrosive painting. However, this kind of traditional rust removing method is very time-consuming. Additionally, it can't always be used conveniently especially for the geometry of location to be treated, e.g. the corner and notch. Now rust converter is commercially available as an alternative to overcome these shortcomings. Rust converter is a liquid metal treatment agent sprayed on rusty surfaces so as to convert the rust into other adherent chemical compounds, thus provides a protective layer and prevents from further corrosion with subsequent coating treatment. Moreover, it reduces labor strength and environmental pollution to a great extent.

Among the rust converters, special attention had been paid to the ones based on tannins and phosphoric acid, while the results on protection efficiency of rust converters were controversial due to several factors, such as the type of acid and its concentration [2-4]. This work presented a new rust converter with formulation based on phosphoric acid. The performance of steel samples with rust or converted layer was investigated by electrochemical characterization i.e. potentiodynamic polarization and electrochemical impedance spectroscopy (EIS) in neutral and acid environment, and the mechanism of effective components in the formulation was discussed.

EXPERIMENTAL SECTION

Reagents for preparation of the designed rust converter were shown in table 1.

Table 1. List of the reagents for rust converter preparation

Reagent	Chemical formula	Mass concentration. %
Zinc oxide	ZnO	0.1~10
Orthophosphoric acid	H ₃ PO ₄	20~40
Potassium dichromate	K ₂ Cr ₂ O ₇	0.5~15
Sodium phosphate	Na ₃ PO ₄	0.5~10
Carbamide	CO(NH ₂) ₂	0.1~10
Water	H ₂ O	50~70

In general, the preparation of the designed rust converter was mainly based on the dissolution of the solid reagents in solvent(water). All the reagents were added into the solvent according to the mass concentration in proper sequence at stirring of the solution with the help of a mechanical stirrer. The duration of reagents dissolution was 20~30 min, and then the rust converter, a transparent or slightly turbid liquid with orange-brown color, was ready for use.

Mild steel samples used in the electrochemical experiment were cut and sealed by epoxy resin with exposure surface (1.0 cm × 1.0 cm) as working electrodes. Then the working surface was polished with SiC abrasive papers, rinsed with distilled water, degreased ultrasonically in ethanol and acetone, and dried in room temperature.

The samples were pre-corroded for 50 days in alternated immersion test (AIT)[4] in 3.5% NaCl solution. After the pre-corrosion stage, friable and powdery rust was brushed off from the surface of the samples with the help of metal brush and then degreased and dried. For half of the samples, high performance rust converter was applied to their surface with brush, and packed layer with dark-grey color was formed on the surface after 12-24 hours.

The electrochemical measurements were performed with PARSTAT 2273 electrochemical workstation(Princeton Applied Research) in a conventional three-electrodes cell system which described elsewhere. The mild steel specimen(rusty or converter treated) and a platinum electrode were used as working electrode and counter electrode, respectively, a saturated calomel electrode (SCE) provided with a Luggin capillary as reference electrode. All potentials were measured versus SCE. The experiment was performed in nondeaerated solutions at 20°C, 30°C, 40°C, 50°C and 60°C, controlled by water bath.

The polarization curves were recorded from -250 to +250mVSCE (versus OCP) with a scan rate of 0.5 mV/s, and the data were collected and analyzed by electrochemical software PowerSuite ver.2.58.

Electrochemical impedance spectroscopy(EIS) measurements were carried out at the open circuit potential (OCP). The ac frequency range extended from 100 kHz to 0.01Hz, and impedance data were analyzed and fitted with ZSimpWin ver.3.21.

RESULTS AND DISCUSSION

In the present study, 3.5% (mass%) NaCl solution and 0.5mol/LHCl solution served as electrolytes, representing for neutral and acid environment, respectively.

Fig. 1 shows the polarization curves of the rusty and converter treated specimens in 3.5% NaCl solution at different temperatures. Corrosion current density (I_{corr}) was deduced by extrapolating the Tafel lines to the corrosion potential. The corrosion inhibition efficiency, %IE_(i), was calculated by equation(1):

$$IE_{(i)} = \frac{i_{corr}^0 - i_{corr}}{i_{corr}^0} \times 100\% \quad (1)$$

where i_{corr}^0 and i_{corr} represented the corrosion current density of mild steel with rusty and converter treated surface. The complete electrochemical parameters E_{corr} , I_{corr} , corrosion rate(v), inhibition efficiency were calculated by polarization measurements and listed in Table 2.

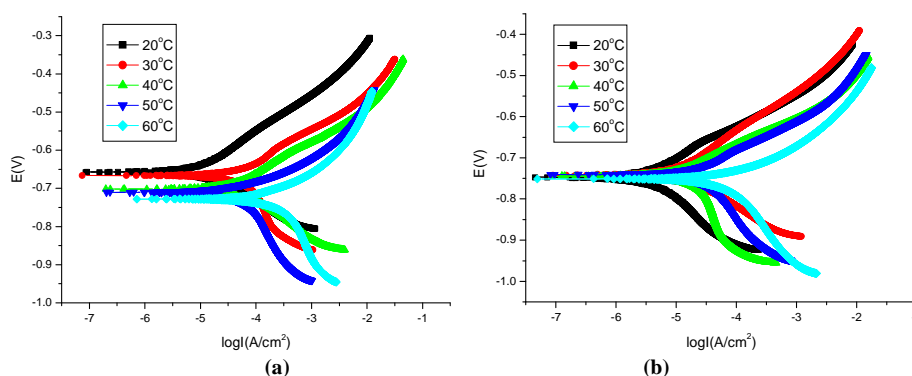
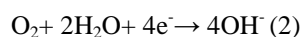


Fig.1 Polarization curves for mild steel (a) with rusty surface and (b) with conversion surface in 3.5% NaCl solution at different temperatures from 20°C to 60°C

Table 2 Polarization parameters for mild steel in 3.5% NaCl solution at different temperatures

Temperature(°C)	Surface State	E_{corr} (mV/SCE)	I_{corr} (mA cm ⁻²)	V (mm a ⁻¹)	%IE _(i)
20	rust	-646.9	0.0218	0.379	-
	conversion	-748.5	0.0031	0.067	85.8
30	rust	-653.2	0.0223	0.469	-
	conversion	-742.1	0.0053	0.114	76.2
40	rust	-708.7	0.0277	0.595	-
	conversion	-744.9	0.0064	0.137	76.9
50	rust	-710.5	0.0362	0.778	-
	conversion	-731.5	0.0070	0.151	80.7
60	rust	-728.3	0.0695	1.494	-
	conversion	-736.3	0.0082	0.176	88.2

It was observed that I_{corr} of mild steel with conversion surface were far lower than that of mild steel with rusty surface in 3.5% NaCl solutions comparatively (Fig.1). The cathodic polarization reaction due to the reduction of dissolved oxygen accorded to the equation (2):



For the rusty samples, the partial cathodic reaction of overall corrosion process on steel in neutral solution was controlled by concentration polarization rather than activation polarization. Compared with the rusty steel, there was an obvious negative shift of E_{corr} , which indicated that the conversion layer generally inhibited the cathodic process of the electrode, meanwhile the presence of the layer resulted in the transition of anodic dissolution from oxygen-diffusion controlled process to electrochemically controlled process. It could be deduced from table 2 that for both rusty steel and conversion layer, the corrosion rate increased with the temperature increasing, and the highest inhibition effect was 88.2, which indicated that the conversion layer could obviously reduce the corrosion rate.

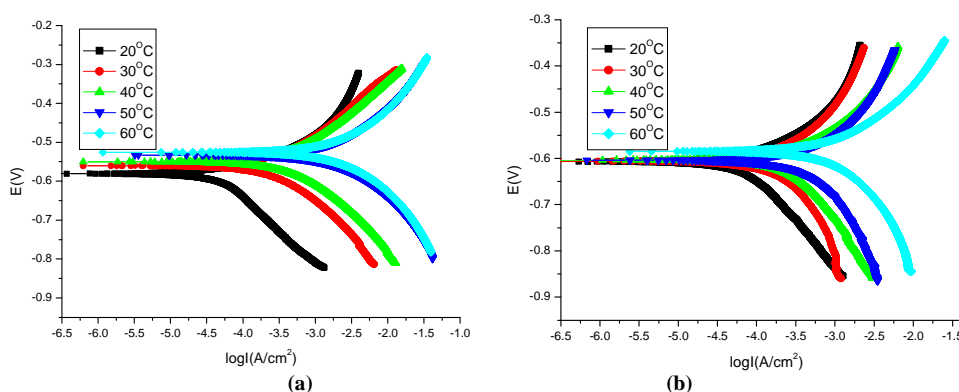


Fig.2 Polarization curves for mild steel (a) with rusty surface and (b) with conversion surface in 0.5mol/L HCl solution at different temperatures from 20°C to 60°C

Fig.2 shows polarization curves of the rusty or converter treated working electrode in 0.5mol/L HCl solution at different temperatures. Also, the complete electrochemical parameters E_{corr} , I_{corr} , corrosion rate(v) and inhibition efficiency were calculated by polarization measurements and listed in Table 3.

Table 3 Polarization parameters for mild steel in 0.5mol/L HCl solution at different temperatures

Temperature(°C)	Surface State	E_{corr} (mV/SCE)	I_{corr} (mA cm ⁻²)	V (mm a ⁻¹)	%IE _(i)
20	rust	-578.5	0.421	9.051	-
	conversion	-612.3	0.104	2.227	74.7
30	rust	-570.2	0.511	10.98	-
	conversion	-610.1	0.150	3.225	70.5
40	rust	-549.9	0.609	13.09	-
	conversion	-606.5	0.172	3.704	71.2
50	rust	-535.7	0.939	20.18	-
	conversion	-607.1	0.197	4.241	79.3
60	rust	-528.0	1.066	22.92	-
	conversion	-594.5	0.209	4.486	80.4

In the aggressive hydrochloric acid solution, the reaction mechanism involved the anodic dissolution of iron and cathodic hydrogen evolution[5]. Despite of the increase of I_{corr} and corrosion rate in comparison with that in neutral solution, the presence of conversion layer simultaneously inhibited the anodic and cathodic process of the electrode, exhibiting a result of mix-controlled process. The increasing temperature also promoted the increase of corrosion rate, illustrating the converter exhibiting its superior value especially in normal conditions as room temperature.

In order to understand the kinetics and mechanism of the film formation on different types of specimens, electrochemical impedance spectroscopic studies were performed.

Nyquist plots for mild steel with rusty and conversion surface in 3.5% NaCl solution at different temperatures from 20°C to 60°C were given in Fig.3. As a whole, the impedance spectra showed a single or an incomplete semicircle and the diameter of semicircle decreased with increasing temperature. For the steel with rusty surface, the Nyquist plots exhibited Warburg type of diffusion lines whereas in the presence of the conversion layer, distorted semicircles were formed. The Warburg lines form different angles with the real component axis, which indicated the radial diffusion of oxygen with concentration gradient located towards the substrate steel. The high frequency distorted semicircles of Nyquist plots were attributed to the faster reactions taking place at the corroding interface (charge transfer of the corrosion process)[6~9].

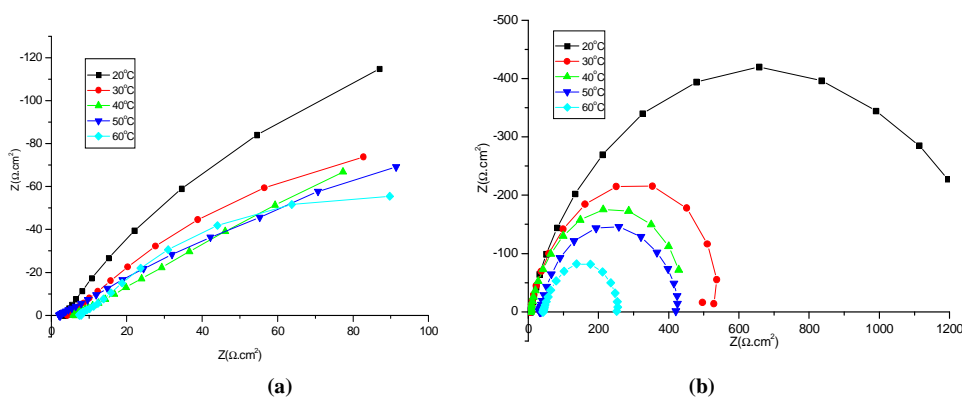


Fig.3 Nyquist diagrams for mild steel (a) with rusty surface and (b) with conversion surface in 3.5% NaCl solution at different temperatures from 20°C to 60°C

The equivalent circuit models used to fit the experimental results were shown in Fig. 4. It consisted of solution resistance (R_s), coating resistance (R_{coat}), charge transfer resistance in the corrosion reaction (R_{corr}), Warburg diffusion resistance (W), constant phase element related to coating capacity (C_{coat}) and electric double layer (C_{dl}).

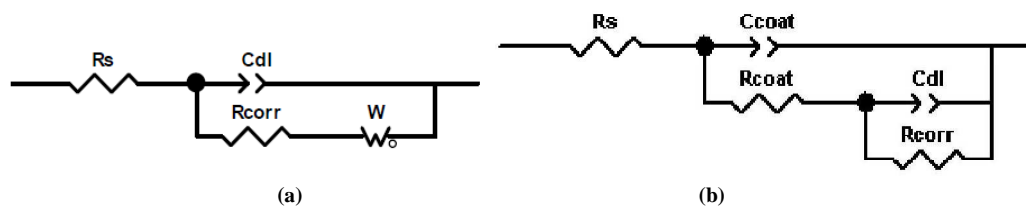


Fig. 4. The equivalent circuit models used to fit the EIS experiment data for steels (a) with rusty surface and (b) with conversion surface in NaCl solution

According to the equivalent circuit, the impedance data were fitted and the electrochemical parameters were given in Table 4.

Table 4 Impedance data of mild steel in 3.5% NaCl solution at different temperatures

Temperature(°C)	Surface State	$R_{corr}(\Omega \text{ cm}^2)$	$R_s(\Omega \text{ cm}^2)$	$R_{coat}(\Omega \text{ cm}^2)$	$C_{coat}(\mu\text{F.cm}^{-2})$	$C_{dl}(\mu\text{F.cm}^{-2})$
20	rust	48.2	5.21	/	/	522.8
	conversion	935.3	6.74	191.9	524.3	202.9
30	rust	39.0	5.34	/	/	384.1
	conversion	428.8	7.47	101.3	292.2	216.6
40	rust	21.2	4.29	/	/	355.9
	conversion	369.1	5.68	57.2	115.4	548.4
50	rust	31.5	5.50	/	/	672.6
	conversion	287.2	8.43	69.1	370.6	337.0
60	rust	33.4	3.82	/	/	371.1
	conversion	178.7	8.11	63.7	303.5	338.9

It could be seen in Table 4 that the R_{corr} values at all investigated temperatures increased markedly in the presence of the conversion layer. And at a lower temperature, e.g. 20°C, the charge transfer resistance reached its highest value of 935.3 $\Omega \text{ cm}^2$, almost 20 times of that for the steel with rusty surface, indicating a remarkable inhibiting effect to corrosion process.

The Nyquist plots consisted of only one capacitive loop in HCl solution both for the steel with rusty surface and conversion layer, as shown in Fig.5. So the equivalent circuit model shown in Fig.6 was used to fit the experimental results. Fitting results were shown in Table 5.

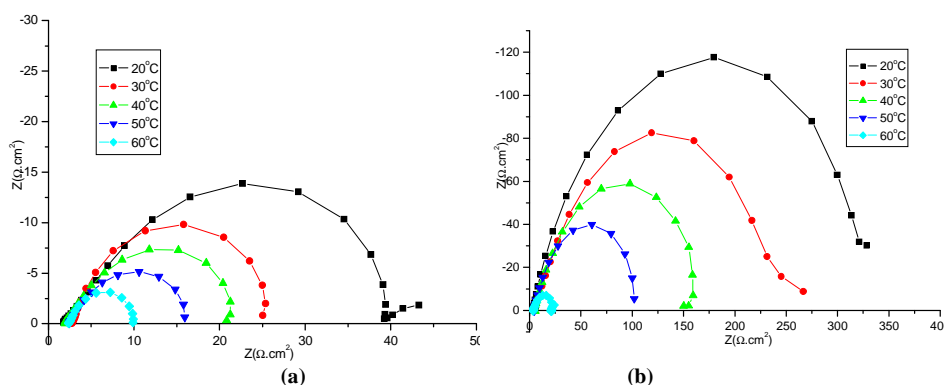


Fig.5 Nyquist diagrams for mild steel (a) with rusty surface and (b) with conversion surface in 0.5mol/l HCl solution at different temperatures from 20°C to 60°C

Table 5 Impedance data of mild steel in 0.5mol/l HCl solution at different temperatures

Temperature(°C)	Surface State	$R_{corr}(\Omega \text{ cm}^2)$	$R_s(\Omega \text{ cm}^2)$	$C_{dl}(\mu\text{F.cm}^{-2})$
20	rust	27.4	2.89	762.7
	conversion	321.2	3.48	499.5
30	rust	21.9	2.31	852.1
	conversion	244.4	2.47	775.8
40	rust	14.5	2.01	920.4
	conversion	162.3	1.68	848.4
50	rust	9.5	2.05	1112
	conversion	100.8	3.43	785.2
60	rust	6.2	2.76	921.6
	conversion	25.7	2.35	767.3

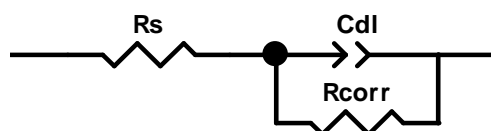


Fig. 6 The equivalent circuit model used to fit the EIS experiment data for steels in HCl solution

The electrochemical experimental studies revealed that the inhibition efficiencies obtained from EIS and polarization were in reasonably good agreement.

Here is some explanation of the mechanism used for the design of rust converter formula. It is a well known fact that the rust formed at steel corrosion includes next phases: hydrated iron oxides such as α -, β - and γ -FeOOH, magnetite Fe_3O_4 (the mixture of two iron oxides: FeO and Fe_2O_3) and amorphous products [10]. Protective phosphate film formed on the corroded steel surface after the usage of the rust converter includes iron(III), chromium(III) and zinc(II) phosphates, according to the results of X-ray analysis (see Fig. 7).

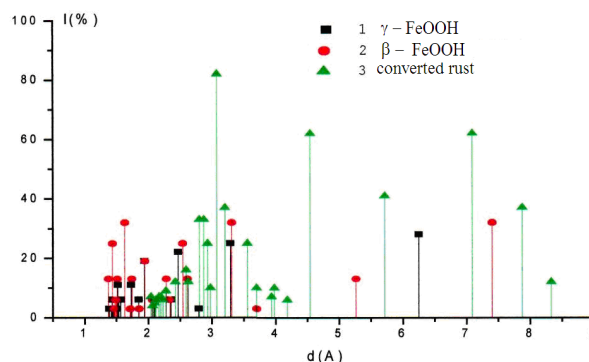
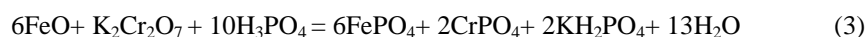


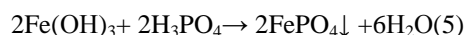
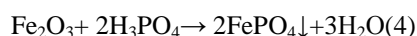
Fig.7. X-ray analysis of the rust(γ - and β -FeOOH) and phosphate film formed in the result of rust conversion

As mentioned above, reagents for the designed rust converter preparation consist of $\text{K}_2\text{Cr}_2\text{O}_7$, H_3PO_4 , ZnO , Na_3PO_4 , $\text{CO}(\text{NH}_2)_2$, etc. Firstly $\text{K}_2\text{Cr}_2\text{O}_7$ oxidizes the iron (II) according to the equation (3):



Iron(III) dihydrogen phosphate– $\text{Fe}(\text{H}_2\text{PO}_4)_2$ and chromium(III) dihydrogen phosphate– $\text{Cr}(\text{H}_2\text{PO}_4)_2$ were formed in condition of acid solution but iron(III) phosphate– FePO_4 and chromium(III) phosphates– CrPO_4 were formed with a high probability in case of the reaction which proceeded on the surface of the steel in outdoor conditions (e.g. neutral environment).

The key reaction between the corrosion products and H_3PO_4 were shown as follows (reaction 4- 5):



Besides, iron(III) dihydrogen phosphate– $\text{Fe}(\text{H}_2\text{PO}_4)_2$ was formed in condition of acid solution but iron(III) phosphate– FePO_4 was formed with a high probability in case of the reaction which proceeded on the surface of the steel in outdoor conditions.

Non corroded metal of the substrate would partly dissolve with the formation of the salt (reaction 6):



However, the presence of zinc ions and chromium in the rust converter led to the isomorphous replacement of iron atoms, resulting in formation of phosphates containing iron ions together with ions of zinc and chromium, as in reaction (7):



Additionally, Na_3PO_4 was used for wetting of the corroded surface and it provided the impregnation of rust converter solution into the corroded surface, and $\text{CO}(\text{NH}_2)_2$ was the inhibitor of the corrosion to prevent the metal of the substrate from excessive dissolution.

Compared with the porous and heterogeneous rust layer, the formation of packed and integrated rust conversion layer provided a protective cover for the steel substrate. The transition from conductor to insulator also minimized the possibility of micro-batteries formation so that the barrier property was improved, the cathodic process was inhibited and the corrosion rate decreased.

CONCLUSION

The studied rust converter show good inhibition properties for the corrosion of mild steel in neutral and acid media, in comparison with untreated rusty steel, and the inhibitor efficiency determined by polarization, EIS were in good agreement. The presence of conversion layer resulted in the transition of anodic dissolution from oxygen-diffusion controlled process to electrochemically controlled process. Due to the increasing of temperature may promote the increase of corrosion rate, the rust converter show its superior value especially in normal conditions as room temperature, The formula of the converter preparation decided the forming mechanism of the packed and heterogeneous conversion layer.

Acknowledgements

The work is supported by Program for International S&T Cooperation Projects of China (2010DFR50860). The support from Postdoctoral Innovation Foundation of Shandong Province and Postdoctoral Scientific Program of Qingdao Enterprises is also gratefully acknowledged.

REFERENCES

- [1] K. E. García, C. A. Barrero, A. L. Morales, *Corros. Sci.* **2008**, 50, 763.
- [2] L. Sorinas, F. Luzardo, T. Ochoa, *Corros. Prot. Mat.* **1997**, 16, 19.
- [3] M. Morcillo, S. Feliu, J. Simancas, *Corros. NACE.* **1992**, 48, 1032.
- [4] J.C. Galvan, S. Feliu, J. Simancas, *Electrochim. Acta.* **1992**, 37, 1983.
- [5] A. Yurta, A. Balaban b, S. Ustun Kandemir. *Mater. Chem. Phys.* **2004**, 85, 420.
- [6] D. D. N. Singh, S. Yadav. *Surf. Coat. Tech.* **2008**, 202, 1526
- [7] S. G. Real, A. C. Elias, J. R. Vilche, *Electrochim. Acta.* **1993**, 38, 2029.
- [8] S. Feliu, R. Barajas, J. M. Bastidas, *J. Coat. Technol.* **1989**, 61, 775.
- [9] C. L. Page, K. W. J. Treadway, *Electrochemical Impedance Analysis and Interpretation*, ASTM, Philadelphia, **1993**, 1188, p.438.
- [10] L. M. Ocampo, I. C. P. Margarit, O. R. Mattos, *Corros. Sci.* **2004**, 46, 1515